Journal of Insect Science, (2020) 20(4): 6; 1–14
doi: 10.1093/jisesa/ieaa055
Review

Review of the EPG Waveforms of Sharpshooters and Spittlebugs Including Their Biological Meanings in Relation to Transmission of *Xylella fastidiosa* (Xanthomonadales: Xanthomonadaceae)

Elaine A. Backus[1,3,4,5,] and Hsien-Tzung Shih[2]

[1]USDA Agricultural Research Service, San Joaquin Valley Agricultural Sciences Center, 9611 South Riverbend Avenue, Parlier, CA 93648-9757, [2]Taiwan Agricultural Research Institute, Applied Zoology Division, Council of Agriculture, 189 Chung-Cheng Road, Wufeng District, Taichung City 41362, Taiwan (R.O.C.), and [3]Corresponding author, e-mail: elaine.backus@usda.gov, [4]Mention of trade names or commercial products in this publication is solely for the purpose of providing specific information and does not imply recommendation or endorsement by the U.S. Department of Agriculture. USDA is an equal opportunity provider and employer.

Subject Editor: Phyllis Weintraub

Received 17 January 2020; Editorial decision 18 May 2020

Abstract

Electropenetrography (EPG) is one of the most rigorous methods to study stylet probing behaviors of piercing-sucking insects whose mouthparts move invisibly inside hosts. EPG is particularly useful for identifying vector behaviors that control transmission (acquisition, retention, and inoculation) of plant pathogens, comparing those behaviors among vector species, and aiding in development of novel vector and disease management tactics. *Xylella fastidiosa* (Wells et al.) is a gram-negative, invasive bacterium native to the Americas, where it is the causal agent of lethal scorch-type diseases such as Pierce's disease of grapevines. *Xylella fastidiosa* is transmitted by sharpshooter leafhoppers (Hemiptera: Cicadellidae: Cicadellinae) and spittlebugs (Hemiptera: Aphrophoridae). Despite over 75 yr of study, details of the inoculation mechanism of *X. fastidiosa* were unknown until the advent of EPG research with sharpshooters. Herein, the following topics are presented: 1) review of key EPG principles and waveforms published to date, emphasizing sharpshooters and spittlebugs; 2) summary of present understanding of biological meanings of sharpshooter waveforms; 3) review of mechanisms of transmission for *X. fastidiosa* illuminated by EPG; and 4) recommendations of the most useful waveform categories for EPG use in future, quantitative comparisons of sharpshooter stylet probing on various treatments such as infected versus uninfected plants, resistant varieties, or insecticide treatments. In addition, new work on the functional anatomy of the precibarial valve is discussed in the context of *X. fastidiosa* transmission and EPG waveforms. Also, the first block diagram of secondary, signal-processing circuits for the AC-DC EPG is published, and is discussed in relation to EPG signals appearances and meanings.

Key words: feeding, stylet penetration, electrical penetration graph

Electropenetrography (EPG) is one of the most useful techniques for studying stylet probing behaviors of piercing-sucking insects and other arthropods whose mouth parts move invisibly inside hosts (history and principles recently reviewed in Backus et al. 2016, 2019). For all types of EPG, a thin gold wire is glued to the dorsum of the insect, and the insect is then placed on an electrified plant. When the stylets are inserted into the plant, the circuit is connected and a constant applied voltage to the plant becomes variable as it passes through the insect. Variable voltages displayed over time produce waveforms that represent fine-scale stylet probing behaviors in the plant. After over 60 yr of EPG studies, we now have several examples where interpreting the biological meanings of EPG waveforms have directly solved formerly intractable problems in understanding transmission (acquisition, retention,

and inoculation) of vector-borne plant pathogens. For example, the biological meaning of the aphid potential drop waveform, which represents intracellular punctures of epidermal and mesophyll cells on the stylets' path to a phloem sieve element, unlocked understanding of the mechanism of acquisition and inoculation of nonpersistent, stylet-borne plant viruses by aphids (Powell et al. 1995, Collar and Fereres 1998, Fereres 2016).

In the Western Hemisphere, sharpshooter leafhoppers (Auchenorrhyncha: Cicadellidae: Cicadellinae) are the most economically important vectors of *Xylella fastidiosa*, the invasive causative bacterium of multiple lethal plant diseases such as Pierce's disease of grapevine, almond leaf scorch, and citrus variegated chlorosis (Purcell 1997, Almeida et al. 2005, Krugner et al. 2019). As described more fully in Backus and Shih (2020), *X. fastidiosa* has recently invaded multiple crops and countries, in part due to spittlebugs (Auchenorrhynhca: Aphrophoridae) as new vectors (Cornara et al. 2017). Recent EPG research has shown that sharpshooter and spittlebug waveforms are nearly identical (Sandanayaka et al. 2007, 2012; Miranda et al. 2009; Backus 2016; Krugner et al. 2019), and have inspired use of EPG with those insects to better understand *X. fastidiosa* transmission and disease management.

Despite over 75 yr of study, details of the inoculation mechanism of *X. fastidiosa* were unknown until the advent of EPG research with sharpshooters. Using primarily *Homalodisca* spp. (Hemiptera: Auchenorrhyncha: Cicadellidae: Cicadellinae) and some others as models, the biological meanings of sharpshooter waveforms have been extensively studied (Backus et al. 2005, 2009; Joost et al. 2006; Dugravot and Backus 2008; Miranda et al. 2009; Cervantes and Backus 2018). Knowledge gained has been used to identify the likely mechanisms of *X. fastidiosa* inoculation. Herein, we will review the following topics to provide background for another paper, Backus and Shih (2020): 1) review key EPG principles and waveforms published to date, emphasizing sharpshooters (primarily) and spittlebugs (secondarily); 2) summarize the present understanding of biological meanings of sharpshooter and spittlebug waveforms; 3) summarize the mechanisms of acquisition and inoculation for *X. fastidiosa* as illuminated by EPG; and 4) recommend the most useful waveform categories for use in future, quantitative comparisons of sharpshooter stylet probing on various treatments such as infected versus uninfected plants, resistant varieties, and chemical treatments.

Summary of the Principles of EPG

History and Types of Monitors

As described in more detail in Backus et al. (2019), EPG was first developed in the early 1960s (McLean and Kinsey 1964) using alternating current (AC) applied signal to the plant and low amplifier sensitivity (or input resistor, Ri) of 10^6 Ohms. Thus, early AC monitors were sensitive primarily to electrical resistance in the aphid to the applied AC signal (now termed the R component) (Backus et al. 2000, 2019; Walker 2000). Fourteen years later, the technology was improved by increasing the Ri level to 10^9 Ohms (Tjallingii 1978), so that both resistance as well as biological voltages or biopotentials (termed the electromotive force or emf component) generated by the aphid-insect interface could be detected. The latter DC EPG monitor (still in use today) applies direct current (DC) to the plant. The originator of the DC system, W. F. Tjallingii, also developed many of the elegant theoretical underpinnings of EPG science, such as the R and emf components (a.k.a. electrical origins of a waveform; Tjallingii 1985a) described herein. Based on Tjallingii's idea of the emf (later renamed R/emf) responsiveness curves, below, a new (AC-DC) monitor design was published 31 yr later (Backus and Bennett 2009). Its purposes were to: 1) unify the differences between the two previous types of monitors, 2) allow researchers to tailor settings to their subject insects, and 3) enable backwards compatibility and comparability of all waveforms generated by any monitor design (Backus et al. 2019).

Design of the AC-DC Electropenetrograph

With the design of the AC-DC monitor, a new naming system for EPG technology also has been introduced (Backus et al. 2019). In keeping with the modern naming system for many other electrical/biological technologies (such as electrocardiography, electroencephalography, and electromyography) the technology of EPG has been renamed 'electropenetrography', still abbreviated EPG. Using the same convention, the instrument is termed an 'electropenetrograph' and the output trace from such a device is termed an 'electropenetrogram'.

The four-channel AC-DC electropenetrograph (EPG Technologies, Inc., Gainesville, FL; andygator3@gmail.com) has selectable Ri levels (amplifier sensitivities) from 10^6 to 10^{10} plus 10^{13} Ohms in the head stage amplifier, allowing users the flexibility to match the inherent resistance of any arthropod of any size. Selectable Ri range also allows researchers to definitively determine proportions of R and emf in each waveform (further described, below), in order to choose whichever Ri level and its waveforms best matches their research objectives. Researchers also can choose either AC or DC applied signal, in order to mitigate any sensitivities the insect (especially those with large body sizes like sharpshooters and heteropterans) might have to applied electricity (Backus et al. 2018a, 2019). Figure 1 shows a simple block diagram for the secondary signal processing circuit of the patented AC-DC instrument, for the first time in print.

The presently available four-channel AC-DC electropenetrograph is similar to the published AC-DC Correlation Monitor (see block diagram, Fig. 1 in Backus and Bennett 2009), but simpler. The Correlation Monitor (no longer available for purchase) had three side-by-side signal processing chains because the instrument was designed to test hypotheses described in Tjallingii (2000) and Backus et al. (2000), especially whether emf could be retained after AC signal processing and the effects of certain circuit elements in the Backus and Bennett (1992) AC monitor. Results from experiments with the Correlation Monitor (Backus and Bennett (2009) showed conclusively that emf could be retained despite AC signal processing. Once issues like use of computerized, high-resolution display of waveforms (using the same, Windaq [Dataq Instruments, Akron, OH] program) and Faraday cage for noise reduction were standardized, the main differences in waveform appearances between older AC monitors and the DC monitor were primarily due to differences in Ri level (10^6 Ohms for AC monitors vs 10^9 Ohms for DC). Backus and Bennett (2009) also showed that coupling capacitors (introduced in the Backus and Bennett [1992] AC monitor to control DC offsets and not exactly the same as filters) caused inversion of aphid potential drops (pd's). Subsequent design work for the four-channel AC-DC instrument removed the coupling capacitors, log amplifier, and two out of three signal processing chains.

Signal processing for the four-channel AC-DC monitor is actually very similar to that of the DC monitor, except that it has a few additional design features that allow it to process AC as well as DC applied signals. After a 1× (unity) buffer amplifier (not shown in Fig. 1 herein), the signal passes through three stages of amplification.

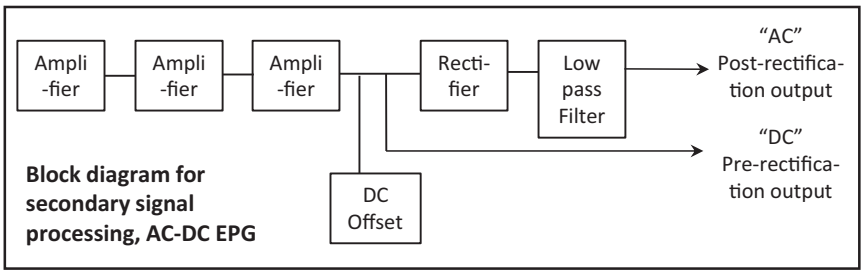

Fig. 1. First published block diagram for the secondary signal processing circuit in the four-channel AC-DC electropenetrograph. See Backus et al. (2019) for the block diagram of the primary, measuring circuit.

When combined with the 100× fixed gain of the head stage amplifier, overall amplification can attain a maximum of 56,661× (accurately calculated via a circuit analysis by IC2 Inc., Gainesville, FL) to enable amplification of even the tiniest emf signals at the lowest Ri level of 10^6 Ohms. The above maximum gain calculation is a correction of previously cited gain of 1,000,000× (Backus et al. 2019), which was based on mistaken calculations.

After amplification, AC carrier wave signals are rectified, meaning that negative signals (i.e., those occurring below 0 V) are inverted or made positive using a precision full-wave rectifier (absolute value extractor, Backus and Bennett 1992, 2009). Importantly, the rectifier precisely removes the entire carrier wave 'perfectly and accurately down to DC (0 Hz)'. Any combination of AC components (fluctuating signals) or DC components (straight upward rises or downward falls) will be 'faithfully reproduced by the circuit', providing complete waveform fidelity to a typical DC monitor output waveform (both previous quotes from Backus and Bennett 2009). A low-pass filter (which is actually part of the rectifier but portrayed separately in Fig. 1 for convenience) then 'draws the envelope' by retaining the peak-to-peak voltages of the positive-only AC carrier wave (Backus and Bennett 1992), restoring the appearance of the insect's waveform despite use of an AC carrier (Backus et al. 2000). The cutoff frequency of the low-pass filter is 80 Hz; therefore, it will not filter out high-frequency emf (according to the Nyquist criterion; Jones 2014), which is estimated to have a maximum frequency of 40 Hz (Backus et al. 2000). The now-normal-looking waveform is output as the 'AC' post-rectification output signal.

To ensure that the post-rectification output has fidelity to published aphid DC EPG waveforms (which have both positive and negative voltage levels; see *Probing Waveform Polarity*, below), a special design feature was added (Backus and Bennett 2009). In brief, after amplification but before rectification, an offset circuit allows up to 4 V of DC to be added to the main circuit well after the measuring point from the insect (i.e., the head stage amplifier); thus, the insect can never feel this current. The DC offset voltage allows the signal to be 'lifted' (using the 'offset' knob; Fig. 2) far above the 0 V axis of symmetry of the following rectifier. Thus, the signal will not be inverted or distorted by the rectifier; it will retain the exact appearance of any negative signal (e.g., the aphid potential drop) because the higher signal will not be inverted or destroyed by the rectifier (Backus and Bennett 2009). A second output plug delivers this 'DC' pre-rectification output signal. Thus, despite only one signal processing chain, each insect has two output waveforms showing signals before and after rectification (Fig. 1). In this way, the user can adjust the offset knob until the two output waveforms look identical, removing any inversion or distortion caused by the rectifier (termed 'restoring native signal polarity' of the waveform; Fig. 2). The offset feature ensures that the outputted waveform from AC applied signal

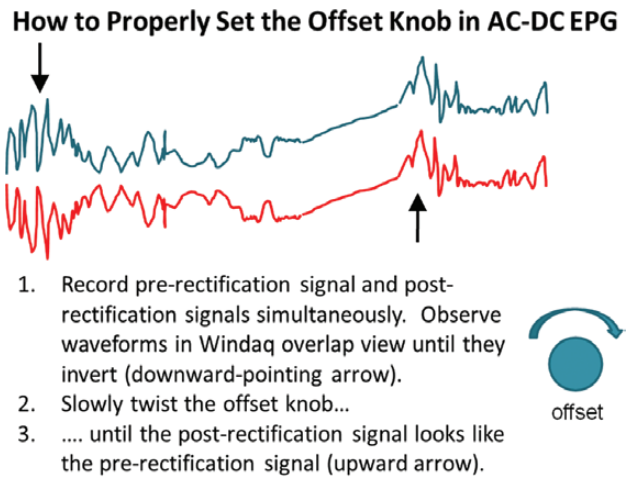

Fig. 2. Explanation of how the offset knob works in AC-DC EPG.

(to the plant) looks identical to what would be outputted using a DC applied signal without rectification.

Accordingly, the secondary signal processing displayed in the block diagram of the four-channel AC-DC electropenetrograph (Fig. 1) is nearly the same as that in the DC monitor block diagram (Tjallingii 2000) but adds the DC offset, rectifier, and low-pass filter. Thus, the AC-DC monitor has been successfully designed to perfectly reproduce the DC monitor output when Ri 10^9 Ohms is used, regardless of AC or DC applied voltage, with the additional capacity to tailor the input resistor (Ri) settings to the study species of choice.

Electrical Origins of Waveforms

Through the performance of targeted experiments (Tjallingii 1985b, 1988; Tjallingii and Esch 1993; Walker 2000; Dugravot et al. 2008), we now understand the behavioral and physiological natures of R (resistance) and emf (electromotive force) components fairly completely. R components are caused by: 1) physical resistance to passage of ionized fluids (the carriers of electrical current in the case of EPG) through the path of fluid taken up by the insect, that is, the insect's buccal cavity or functional foregut (that is, combined stylet food canal, precibarium, and cibarium), or 2) electrical conductivity of such fluids. Thus, R components occur in response to and are directly dependent on the amount of applied voltage/current. Examples of R components generated through electrical resistance to current flow include opening and closing of valves and/or pumps in the buccal cavity. Examples of R components generated through electrical conductivity are highly conductive sheath saliva versus dilute, poorly conducting plant sap.

In contrast, electromotive force components (a.k.a. biopotentials) are completely independent of applied voltage. These tiny voltages are generated internally by properties of the interaction between the plant and stylets, such as stylet breakage of electrically active plant cell membranes (Tjallingii 1985b, Walker 2000), or streaming potentials generated by charge separation of ionized fluids moving through tiny capillary tubes (like the stylet canals) (Walker 2000, Dugravot et al. 2008, Backus et al. 2019). Thus, an example of an emf-dominated waveform caused by membrane breakage is the aphid potential drop waveform described in the first paragraph of this paper. An example of an emf waveform caused by streaming potentials is the ingestion waveforms of many insects; this waveform is caused by rapid pumping for fluid uptake.

In reality, almost all waveforms (including all above examples) are composed of a mixture of R and emf, in different proportions depending upon the biological meaning of the waveform (Backus et al. 2019). For example, a theoretical pathway waveform representing salivation (combined sheath and watery saliva) would have an R component from the electrical conductivity of various types of proteinaceous saliva, but also an emf component from liquid saliva moving in and out of the stylets via pumping of the (tiny) salivarium. This small emf would be combined with (in sharpshooters) larger emf from streaming potentials generated by alternate uptake and egestion of a plant-fluid-plus-saliva mixture brought into the buccal cavity by pumping of the larger cibarium. Thus, the waveform represents a complex gestält of chemical/biological processes occurring simultaneously or progressively during two-way fluid flow through two stylet canals (food and salivary). The largest challenge for interpreting and defining waveforms is to tease apart multiple meanings blended together in a single waveform output. R and emf components of waveforms are our most important electrical tools to meet this challenge of interpretation (Tjallingii 1988, Backus et al. 2019). Interestingly, each amplifier sensitivity (Ri level) can detect a different fraction of the R or emf components present in a waveform. The relationships between Ri level, R, and emf are portrayed in R/emf responsiveness curves.

R/emf Responsiveness Curves

As first hypothesized by Tjallingii (1978, 1985a, 1988) and described in Backus et al. (2019 [both main paper and supplemental information online]), each insect species is thought to have a unique, sigmoidal responsiveness curve that describes the proportions of R and emf that are detectable in its waveforms when they are recorded at each Ri level. As Ri level is increased, proportion of the detected signal that is composed of emf increases, while proportion of R decreases (Fig. 3, y-axis labels). At Ri 10^{13} Ohms, nearly 100% (asymptotically) of any waveform depicted in the output signal is due to emf; at Ri 10^{6} Ohms, the waveforms are nearly 100% R (again asymptotically). Intermediate Ri levels (i.e., 10^{7}, 10^{8}, 10^{9}, and 10^{10} Ohms) show intermediate proportions of R and emf. Each arthropod species has an inherent resistance (termed Ra). The fixed proportion of the inherent resistance (typically, the exponent, such as 10^{6} or 10^{9}) will depend upon the size of the insect (and therefore, roughly the diameter of its food and salivary canals in the stylets). The numerically fluctuating portion of Ra will depend upon the behaviors performed (i.e., the R component of each waveform). At the fixed Ra level, each arthropod has a unique, intermediate Ri level that will represent the 50:50 R:emf proportion for that species (Backus et al. 2019). At that Ri level (i.e., when Ri = Ra), the maximum number of waveforms will be displayed because all R and emf components will be visible and balanced.

The original R/emf responsiveness curve was described for aphids by Tjallingii (1978, 1985a, 1988), by which it was determined that Ri 10^{9} Ohms represented the best approximation of 50:50 R:emf for average-sized aphid species, and therefore 10^{9} Ohms was chosen for the fixed Ri of the DC monitor (Tjallingii 1988). Tjallingii's measurements of amplifier responsiveness for smaller and larger aphids suggested that the curve moves to the left (Fig. 2) as aphid body size increases (i.e., to 10^{8} Ohms) or to the right as body size decreases (i.e., to 10^{10} Ohms) (Tjallingii 1985a). Based on these findings, Backus hypothesized that even larger, nonaphid hemipterans such as sharpshooters and heteropterans would require Ri levels lower than 10^{9} Ohms to display maximum detail in waveforms (Fig. 3, dashed lines) (Backus et al. 2019). Accordingly, selectable Ri levels were developed

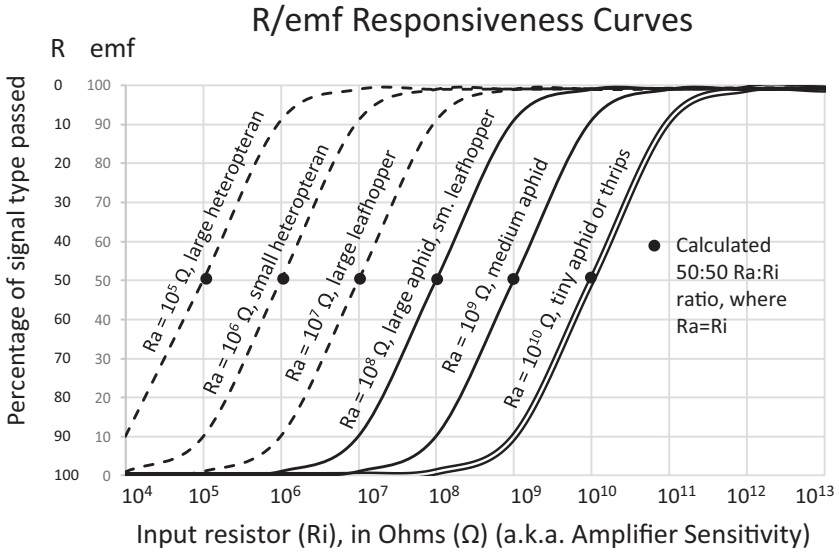

Fig. 3. R/emf responsiveness curves resulting when the percentage of signal type/electrical origin (R or emf) is graphed over Ri levels (amplifier sensitivity). Responsiveness to emf is represented by most lines; Tjallingii's calculation of R responsiveness is drawn parallel to the emf line for Ra = 10^{10} Ohms. Data on aphid curves is from Tjallingii (1988) (solid lines) supplemented by hypotheses of Backus for other insects (dashed lines). Suggested interpretations of Ra levels for emf responsiveness are written parallel to lines. See text herein and Backus et al. (2019; both narrative and supplemental information) for further explanation.

for the AC-DC electropenetrograph so that researchers could attempt to tailor the Ri level to the fixed Ra for any arthropod size recorded, thus expanding the usefulness of EPG to any arthropod.

Selectable Ri levels also can be used to create a waveform library, that is, a series of waveform images that demonstrate how a given species' waveform appearances change at each of several Ri levels. By comparing relative amplitude of a waveform across Ri levels, one can determine how much R and emf, relatively, are detected at each Ri level (Backus et al. 2013, Pearson et al. 2014, Cervantes et al. 2016, Lucini et al. 2016, Cervantes and Backus 2018, Backus and Shih 2020). One can then identify R- or emf-dominated waveforms. When combined with the order of progression when each waveform occurs, one can erect testable hypotheses for the meanings of that waveform. Actual data to construct R/emf responsiveness curves for insects other than aphids (in the same manner as Tjallingii 1978, portrayed in Fig. 3) have not yet been gathered. Consequently, the best evidence to date for a leftward shift in responsiveness curves for large insects is from waveform libraries. Because biological mechanisms of R and emf are now fairly well understood (see above) (Walker 2000, Backus and Bennett 2009, Backus 2016) the process of defining and interpreting a waveform can be sped up by identifying its R and emf components via waveform libraries.

Probing Waveform Polarity

Whether an EPG-recorded stylet probe is biphasic or monophasic (Tjallingii 1985a) has been termed a probing waveform's polarity (Backus 2016). Waveforms that together represent a stylet probe can 'ride' at certain voltage levels in relation to the baseline. The baseline is the flat voltage level (often but not always near 0 V), when the insect is standing still on the plant without stylet probing. A probe's waveforms are biphasic when the initial change from baseline is either a steep rise or drop, then the following waveforms occur both above and below baseline level (Fig. 4A). A probe's waveforms are monophasic when a steep rise occurs at the beginning then the following waveforms ride wholly above the baseline (monophasic positive) (Fig. 4C) or a steep drop occurs then they ride wholly below the baseline (monophasic negative) (not shown). Waveforms can also be described as positive-going or (positive-oriented) or negative-going (or negative-oriented) to describe which direction the peaks point; upward (positive) or downward (negative). This directionality depends upon whether the applied signal to the plant is positive (+DC or AC) or negative (–DC), respectively. The individual peaks of R-component waveforms can be positive-oriented regardless of whether the probe is biphasic (Fig. 4B) or monophasic positive (Fig. 4D).

The biological meaning of biphasic polarity was first described for aphids, when it was demonstrated that stylet tips were accurately correlated with specific cell types for positive voltage level and negative voltage level. Positive voltage level in biphasic aphid probes means stylet tips are in extracellular, usually apoplastic space in the plant (e.g., inside positively charged cell walls or mature [dead] xylem cells). Negative voltage level means stylet tips are in symplastic space (negatively charged living cells) (Tjallingii 1985b, Spiller et al. 1990, Tjallingii and Esch 1993, Walker 2000). In this case, the stylet tips are acting like an intra-/extracellular electrode to detect the electrical voltages in their immediate vicinity in the plant. Generally, biphasic waveforms demonstrate steady, flat voltage levels either above baseline (termed extracellular level) or below baseline (termed intracellular level). Biphasic polarity is a strong emf component (in fact, the first one discovered; Tjallingii 1985b) and, thus, is best detected at high Ri level, especially 10^9 Ohms or higher. Accordingly, biphasic polarity (and thus the high Ri level that generates it) can be valuable because it provides definitive information about intracellular versus extracellular stylet tip locations in a plant.

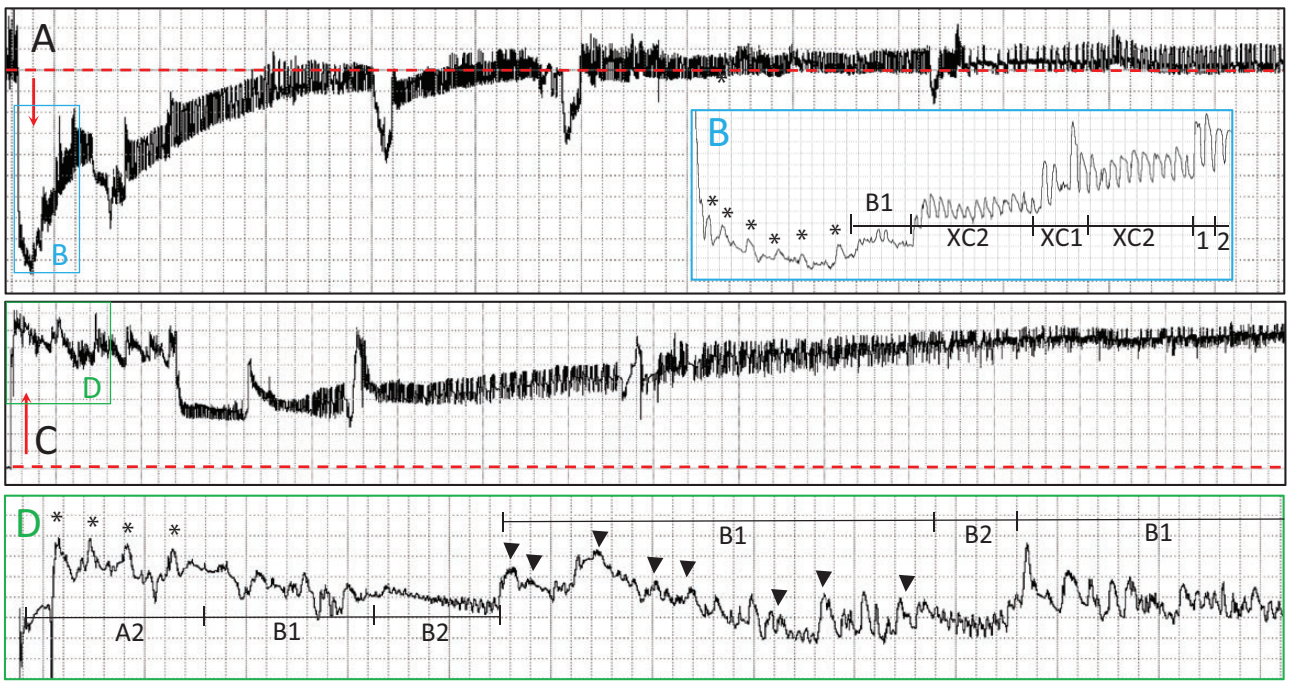

Fig. 4. Compressed examples of probing waveform polarity with certain sections expanded; from previously unpublished waveforms of *G. atropunctata*. (A) Biphasic waveforms recorded using Ri 10^9 Ohms and 50 mV AC applied signal. (B) Expansion of pathway waveforms from box labeled B in part A. (C) Monophasic positive waveforms using Ri 10^7 Ohms and 200 mV AC applied signal. (D) Expansion of pathway waveforms from box labeled D in part C. Windaq compression of parts A and C is 50 (10 seconds per vertical division). Windaq compression of parts B and D is 3 (0.6 seconds per division). Windaq gain is 16× in parts A and B, 4× in parts C and D. *A2 peaks, positive-oriented. Dashed lines (red in online version, gray in print version) represent baseline.

Voltage level becomes primarily monophasic positive (assuming applied voltage is +DC or AC) at lower Ri levels, especially 10^6 Ohms, in virtually all hemipterans studied to date. This observation includes aphids (Backus and Bennett 2009), leafhoppers (Carpane et al. 2011, Chuche et al. 2017), sharpshooters (Miranda et al. 2009), and heteropterans (Backus et al. 2013, Cervantes et al. 2016, Lucini et al. 2016). Monophasic polarity is usually an indication of strong R components in the waveforms. Monophasic waveforms are not steady in voltage level but rise and fall through undulations that have been histologically correlated with stylet protractions and retractions through various depths in the plant tissue (Backus et al. 2005, Joost et al. 2006). Such undulations are particularly evident during pathway phase (Fig. 4C) when the insect is seeking a cell for ingestion, protracting and retracting the stylets as it searches. It has been hypothesized that applied voltage (thus contributing to R components) becomes stratified in a plant, being higher in the outer layers and much lower in inner layers of larger, more watery cells such as xylem or pith (Backus 2016). Thus, the stylet tips of all hemipterans detect larger, grosser electrical voltages in the plant at lower Ri levels than at higher Ri levels, allowing interpretation of behaviors such as large stylet movements and depth in the plant. Interestingly, waveforms recorded at intermediate Ri levels like 10^7 and 10^8 Ohms can be either biphasic or monophasic, according to the size of the insect, type of adhesive used, and the quality of wiring job (thus, degree of conductivity of signal) (Cervantes and Backus 2018).

Sharpshooter and Spittlebug EPG

Species Recorded

The blue green sharpshooter, *Graphocephala atropunctata* (Say) (previously *Hordnia circellata* (Baker)) was the first-ever leafhopper species to be recorded via EPG (Crane 1970, summarized in Almeida and Backus 2004). Several aspects of waveform names and biological meanings continue to be useful from that early paper. Starting in 2004, extensive modern EPG research has been performed with multiple sharpshooter species, primarily from the Western Hemisphere. Overall similar EPG waveform appearances have been found for *G. atropunctata*, as well as glassy-winged sharpshooter, *Homalodisca vitripennis* (Germar), smoke tree sharpshooter, *H. liturata* Ball (all North American species), and *Bucephalogonia xanthophis* (Berg) (South American, Brazilian) (all waveforms and papers summarized in Table 2 in Backus 2016, and listed below). Additionally, recent research with spittlebug vectors of *X. fastidiosa* show that these insects perform waveforms nearly identical to those of sharpshooters (at least in coarse- and medium-resolution appearance, as judged by published figures). Studied species include the cosmopolitan meadow spittlebug, *Philaenus spumarius* (L.) (Cornara et al. 2018), and endemic New Zealand spittlebug, *Carystoterpa fingens* (Walker) (Sandanayaka et al. 2007, 2012). It is also possible that some waveform appearances of sharpshooter/spittlebug recordings could be seen in those of other leafhopper species as well, especially at high Ri levels, because sharpshooter-like X waves are documented from *Scaphoideus titanus* Ball, a deltocephaline grape leafhopper introduced from North American and common in European vineyards (Chuche et al. 2017).

Waveform Libraries

The first waveform library for sharpshooters (Cervantes and Backus 2018) used R and emf components to define all waveforms for *G. atropunctata*, and also corroborated previous correlational research using histological and artificial diet methods (Backus et al. 2005, Joost et al. 2006, Dugravot et al. 2008). Cervantes and Backus (2018) also demonstrated how the appearances of sharpshooter waveforms can vary with different wiring methods, wire adhesives, and applied voltages. The second sharpshooter waveform library is now published (Backus and Shih 2020), for *Kolla paulula* Matsumara, the first Asian sharpshooter to be EPG-recorded.

Waveform Polarity

Sharpshooter stylet probes recorded at high Ri levels often begin at a negative (intracellular or symplastic) level during pathway, but gradually rise into positive voltage level (extracellular or apoplastic) after their stylet tips become strongly anchored into a mature (dead) xylem cell (Backus 2016, Cervantes and Backus 2018). Thus, for sharpshooters, biphasic polarity is seen at 10^9 Ohms, but in reverse (negative proceeding into positive voltage levels) compared with aphids (positive proceeding to negative) because sharpshooters and other auchenorrhynchans perform intracellular stylet penetration, that is, stylet tips move directly through cells during pathway, instead of around them through cell walls, as do those of aphids. At 10^6 and 10^7 Ohms, all sharpshooter waveforms are monophasic positive, with voltage levels above the baseline varying indirectly with the stylet depth in the plant; the lower the voltage level of the pathway waveform, the deeper the stylets are penetrated into the plant (Backus et al. 2005, 2009). Probing waveform polarity varies between biphasic and monophasic positive for 10^8 Ohms, depending on quality of wiring (Cervantes and Backus 2018).

Waveform Naming Conventions

Previously established conventions of EPG terminology (Backus [2016] and Cervantes and Backus [2018]) are used herein and in Backus and Shih (2020). In brief, an uninterrupted stylet insertion into the plant is synonymously termed a stylet probe or stylet penetration (Backus 2000). An individual occurrence of an uninterrupted waveform is a waveform event (Backus et al. 2007, Ebert et al. 2015). The Backus convention for sharpshooter waveforms is used herein, which is based on earlier work (Crane 1970, Almeida and Backus 2004) and then was used in eight additional sharpshooter papers studying the species listed above (Backus et al. 2005, 2009; Joost et al. 2006; Dugravot et al. 2008; Sandanayaka and Backus 2008; Backus and Morgan 2011; Cervantes and Backus 2018; Krugner et al. 2019). The Backus naming convention was also applied to *C. fingens* spittlebugs (Sandanayaka et al. 2007). Subsequently, a different waveform naming convention was developed for *B. xanthophis* sharpshooter (Miranda et al. 2009), which was recently applied to *P. spumarius* spittlebug (Cornara et al. 2018). The Miranda convention is synonymized with the Backus convention herein (in parentheses after each Backus waveform name in the narrative, and in a separate column in Table 1).

In the Backus convention, waveforms are named hierarchically. The waveform phase is the name for a coarse (compressed) level of resolution (Fig. 4A and C), which broadly describes large categories of stylet penetration such as *pathway* and *sustained ingestion*. At slightly increased resolution, waveform families such as A and B can be distinguished within each phase. Further increases in resolution reveal fine-structure, high-resolution information, categorized as waveform types (Fig. 4B and D) and subtypes. Types are denoted by the family's uppercase letter followed by a number, for example, B1, while a subtype is denoted by an added lowercase letter, for example, B1w. This hierarchical convention based on electrical appearance

Table 1. Summary of the most important sharpshooter (and spittlebug) waveforms, categories, and biological meanings from research to date

Waveform categories and names (Backus)			Synonym (Miranda)	Biological meanings	
Phase Family	Type	Subtypes		Stylet tip location	Stylet, foregut [and transmission] activities
T[a]			C	Epidermal/parenchyma	Test probe [may inoculate some bacteria into epidermal or upper mesophyll cells]
Pathway (**P**)				Nonxylem cells	Vigorous stylet movements and sheath (gelling saliva) secretion to form the salivary sheath to a mature xylem cell.
A	A1, A2			Epidermal/outer mesophyll or parenchyma	Initial stylet insertion (A1) and formation of sheath trunk and early branches by full stylet bundle (A2).
B	B1	B1s, B1w, **B1p**[a]		Mesophyll/parenchyma, immature xylem cell	Multiple sheath branches extended by maxillary stylets only. Mix of saliva and fluid taken up and swished around buccal cavity for tasting. Rinsing egestion. [Likely inoculates bacteria into mesophyll and abandoned, immature xylem cells]
	B2			Mesophyll/parenchyma after leaving mature xylem cell	Stylet chiseling through solid wall of sheath after abandoning an unacceptable xylem cell and retracting or extending stylets; new branch formed.
X wave					
XN	XB1[b]	XB1s, fB1w	N	Mature xylem cell	Same as pathway B1, but in a xylem cell; saliva/fluid uptake, tasting, rinsing egestion. [Inoculation of bacteria into xylem cell]
XC	**XC1**		Xc	Mature xylem cell	Uptake of saliva/fluid mix, rapid spitting out; discharge egestion. [Inoculation of bacteria into xylem cell]
	XC2		Xi		Trial ingestion to test strength of salivary seal.
Sustained ingestion					
C	**C2**		Xi	Mature xylem cell	Sustained ingestion (active cibarial pumping and swallowing into pharynx, esophagus then midgut) [Acquisition of bacteria into functional foregut]
G				Mature xylem cell	Proposed fluid sips for tasting/testing, interspersed with stylets resting in xylem cell.
Interruption					
N			N	Mature xylem cell	Interruption of sustained ingestion for tasting/salivation [may inoculate bacteria?]
Others					
D	D1, D2			Unknown (cellular?)	Unknown, possibly stylets moving slowly.
R				Any tissues (shallow?)	Resting with stylets inserted into xylem (C/G voltage level) or epidermis (just above baseline).
SR				Any tissues	Rapid stylet withdrawal from and re-insertion into same salivary sheath.
W			W	After leaving mature xylem cell	Rapid withdrawal of stylets from xylem cell and plant, with salivation.

Waveform naming convention is that of Backus and colleagues (Backus et al. 2005, Backus 2016). The separate naming scheme used in Miranda et al. (2009) and Cornara et al. (2017) is synonymized. For more details, see Table 1 in Cervantes and Backus (2018). Underlined Backus names are recommended for measurement of waveforms for quantitative comparison studies.

[a]See Backus and Shih (2020) for more information on T and B1p and why we recommend measuring them in quantitative studies.

[b]This waveform type was mistakenly referred to as B1 in Cervantes and Backus (2018). We correct that error herein.

allows flexibility for future, quantitative studies. Initially complicated names can now be simplified based on subsequent, post-naming research findings on meanings of waveforms. Thus, a rational choice of waveform detail for quantitatively measuring recordings can now be chosen, as demonstrated at the end of this paper.

Sharpshooter Waveforms and Their Biological Meanings

This summary is taken from detailed descriptions in Backus (2016), Cervantes and Backus (2018) and summarized more briefly in Krugner et al. (2019). Key correlational findings supporting the biological meanings of these waveforms are also summarized from the eight other papers cited above. See Cervantes and Backus (2018), Table 1, for much more detail.

Pathway Phase (Miranda C)

Pathway represents the process of searching for and finding a xylem cell for sustained ingestion. A key behavior during pathway is obligate formation of a dense salivary sheath to the xylem cell. Pathway phase comprises families A and B.

Family A

This is the highest-amplitude waveform, at the beginning of each probe, representing secretion of the salivary flange and first insertion of the full stylet bundle to form the trunk of the salivary sheath. It also represents the limit of penetration of the mandibular stylets (Joost et al. 2006). Family A can be composed of types A1 or A2, or both.

Type A1

A1 is the waveform with the highest relative amplitude in the entire probe and is especially tall compared with the lowest-amplitude waveform, C2 (at low Ri levels) or B1 (at high Ri levels) (see below). A1 is composed of one or two tall, thin peaks, is heavily R-dominated, and is often absent at higher Ri levels.

Type A2

This waveform, if present, immediately follows A1 and appears to be a transition between A1 and B1 (see below). A2 usually slopes downward (Fig. 4B and D, asterisks) as the stylets push deeper into the plant). At lower Ri levels, distinct peaks similar to A1 but shorter can often be seen. At higher Ri levels or with poor wiring or silver paint, A2 becomes amorphous. Thus, A2 is R-dominated. A2 can be interspersed with short voltage drops (vd's) of unknown meaning (Backus et al. 2005, 2009) (not shown herein, but shown in Backus and Shih 2020). These vd's were previously termed pd's in Cervantes and Backus (2018), but their name is changed herein and in Backus and Shih (2020) to reduce comparison with the aphid potential drop waveform. Like aphid pd's, sharpshooter vd's might represent brief cell membrane breakages until mixing of previously compartmentalized compounds causes loss of charge separation (Backus 2016). However, unlike the aphid potential drop waveform, vd's are R-dominated because they disappear at high Ri levels.

Family B

The lower-amplitude, variable-appearance waveforms that form the bulk of pathway phase are family B. This complex family represents deeper penetration of the maxillary stylets alone, through the mesophyll/parenchyma tissues into the vascular bundle with secretion of one to several salivary sheath branches (Backus et al. 2005, 2009; Joost et al. 2006).

Type B1

Evidence described below supports that B1 (Fig. 4B and D) represents fluid movements that mediate tasting and testing contents of cells along the pathway, and also in small, immature xylem cells that are rapidly rejected and abandoned. Sometimes a 'partial X wave' (see below) is recognizable in B1 (depending upon the sharpshooter species), but often not (Backus et al. 2009). Like A2, B1 can also include very brief vd's when viewed at low Ri level. B1 is composed of long sequences of alternating subtypes B1w and B1s (see descriptions below), forming the bulk of pathway phase in both sharpshooters and spittlebugs (see magnified insets of figures in Miranda et al. 2009 and Cornara et al. 2017). B1 is likely a balance of both R and emf components (Cervantes and Backus 2018). Many complicated stylet and cibarial pump movements likely occur during B1, described below.

B1: Subtype B1w

This is the wave-like portion of B1 (Fig. 4B and D). Joost et al. (2006) observed secretion of a blob of mixed sheath and watery saliva during B1w.

B1: Subtype B1s

This is the spikelet burst portion of B1 (Fig. 4D, downward arrowheads). Spikelet bursts occur at all Ri levels for all species; therefore, they are caused by a mixture of R and emf components. Spikelets can either ride on top of short plateaus, especially at higher Ri levels as with *G. atropunctata* (Cervantes and Backus 2018) (Fig. 4D), or be relatively flat on the same voltage level as B1w, especially at lower Ri levels with larger sharpshooters, as with *Homalodisca* spp. (Backus et al. 2009). Therefore, the rise and fall of the plateau is an emf component. Frequency of the spikelet burst is different from that of visible, co-occurring fluttering of the stylet tips, or any other movements of mouthparts. No sheath salivation is observed during B1s. Therefore, the spikelet burst is hypothesized to represent some internal process controlling in-out fluid movements (Joost et al. 2006).

Because of their small amplitude, spikelets likely represent movements of tiny amounts of fluid (see discussion of streaming potentials, below). Due to the small size of the precibarium, these tiny volumes are probably moving into and out of that canal. Small fluid movements are hypothesized to be caused by two (potentially interacting) mechanisms (Backus 2016). In summary, the first possible mechanism is minor (partial), tiny-amplitude, up-down movements of the cibarial diaphragm (termed 'cibarial quivering') (E.A.B., personal observations) for which there is as yet no published evidence except an understanding of electrical origins of B1s and streaming potentials by Dugravot et al. (2008), below. The second possible mechanism is turbulence in the distal precibarium caused by movements of the precibarial valve, evidence for which is based on functional anatomy, fluid dynamics studies, and bacterial colonization. Multiple published lines of evidence support expulsion of small volumes of fluid (termed 'rinsing egestion') from the precibarium. Because rinsing egestion is proposed to be one of two likely mechanisms of inoculation of *X. fastidiosa* bacteria, it is worthwhile to review in some detail the nature of the evidence for rinsing egestion summarized above. The present review is an update of the ideas presented in Backus (2016) and Krugner et al. (2019).

Cibarial quivering is supported by the existence of streaming potentials, an idea first proposed by Tjallingii (1978), explained by Walker (2000), and eventually proven by Dugravot et al. (2008). Streaming potentials spontaneously develop when electrically charged fluids are pulled rapidly through a very narrow capillary tube, like the food canal (Walker 2000, Backus et al. 2019). Dugravot

et al. (2008) used a combination of cibarial videomicrography, electromyography, and EPG to demonstrate that the emf-dominated voltage rise of the sharpshooter waveforms now termed XC1 and XC2 (described below) is generated when fluids are pulled through the precibarium into the cibarium by major uplift of the cibarial diaphragm. The subsequent emf-dominated fall in voltage is caused by full release of the diaphragm and reversal of fluid flow out of the cibarium. Absolute amplitude of the resulting voltage peak (XC1) or plateau (XC2) is directly related to degree of uplift of the cibarial diaphragm, thus volume of fluid taken up (Dugravot et al. 2008). It has been proposed (Backus 2016) that, in similar fashion, very tiny to medium-sized, up-down peaks (i.e., B1s spikelet bursts and B1p peaks [see below], respectively) likely represent cibarial quivering to bring smaller volumes of fluid into the precibarium then expel them. Thus, R and emf components of B1s suggest an initial small uptake of fluid during the rise of the short plateau (emf), followed by rapid, in-out movements from the stylet tips (R plus emf) of tiny amounts of fluids during the burst, followed by more complete expulsion during the fall of the plateau (emf).

Possible valve-related turbulence is supported by several studies of functional anatomy, chemosensory function, and fluid dynamics. Recently, Ruschioni et al. (2019) used elegant light microscopy, transmission electron microscopy (TEM), and scanning EM (SEM) to update the previous work of Backus and McLean (1982) to identify a new type of closure mechanism for the valve and further support that turbulent fluid flow is likely in the precibarium below (distal to) the valve. Ruschioni et al. (2019) visualize the interior anatomy of the area surrounding the precibarial valve of *P. spumarius*. This anatomy may be similar to that of sharpshooters based on nearly identical appearances of structures visualized with SEM (Backus and McLean 1982, Backus 1988) and confocal microscopy (Backus and Morgan 2011). Ruschioni et al. (2019) discovered a bell-like invagination interior to a structure called the precibarial pit by Backus and Morgan (2011) and the (precibarial) ring by Ruschioni et al. (2019). Backus and McLean (1982) hypothesized that the pit/ring was the opening of an apodeme attached directly to the valve muscle, and that the adjoining flap was levered across a nearby procuticular fulcrum such that, when the muscle/apodeme contracted, the flap would lever up to close against a lip on the opposing side of the precibarium. The new findings of Ruschioni et al. (2019) instead show that spittlebug precibaria have no obvious fulcrum, the muscle is not directly attached to the flap of the valve, the flap is not levered, and the pit/ring is the opening of the bell-like invagination to which the valve muscle actually attaches. The interesting interpretation of Ruschioni et al. (2019) for the closure of the valve is that relaxation of the muscle partly closes the flap, but that fluid taken up into the distal precibarium fills the bell-like invagination to complete the closure of the flap flatly against the hypopharynx.

It could be argued that evidence for flat closure of the flap is not presented in Ruschioni et al. (2019). Their TEM images (especially Figs. 1C and 2A) show the flap touching the hypopharygeal surface at angles similar to those envisioned by Backus and McLean (1982). This suggests more structural flexibility in the flap than envisioned in the stylized drawing in Fig. 3 of Ruschioni et al. (2019). Such flexibility may contribute to fluid turbulence in the distal precibarium, in addition to that of proposed mixing of fluids into and out of the bell-like invagination. Nonetheless, the rest of the evidence presented by Ruschioni et al. (2019) matches their interpretation that no independent muscular action occurs to close the precibarial valve, only to open it. In addition to the role of the bell-shaped invagination in valve closure, it is likely that cuticular elasticity also contributes to closure. Cuticular elasticity appears to be the primary closing mechanism of the cibarial pump, which also lacks an antagonistic muscle for closing (Dugravot et al. 2008). Accordingly, all evidence combined supports that the resting position of the precibarial valve of spittlebugs (and perhaps also leafhoppers/sharpshooters) is tight closure, similar to the ball-and-socket-like valve of aphids and psyllids (Ullman and McLean 1986).

Nonetheless, turbulence distal to the valve was also found in a recent fluid dynamics study modeling flow through the precibarium of hypothetically bacteria-free *G. atropunctata* (Ranieri et al. 2020). In that work, *X. fastidiosa* colonization hypothesized for the length of the precibarium caused increased turbulence throughout the channel, but especially below the valve (Ranieri et al. 2020). Such turbulence probably scrubs off colonizing bacteria in the distal portion of the precibarium, as demonstrated in a confocal microscopy study of precibarial colonization (Backus and Morgan 2011).

Closure at rest is further supported by chemosensory functions of the sharpshooter precibarium. Cutting the nerves for only the distal (D) chemosensory papillae located distal to the valve completely abolishes the ability of *G. atropunctata* to taste different concentrations of sucrose infused into plants, despite the existence of proximal (P) chemosensilla located above the valve (Backus and McLean 1983). Abolition of chemosensory function supports a two-stage sensory process (Backus and McLean 1982). First-stage chemosensing of incoming fluid is performed by the D sensilla while the valve is closed (at rest), after which the valve must be actively opened for second-stage chemosensing of the fluid by the P sensilla above the valve. Chemosensation of compounds interior to the plant occurs during pathway phase when the insect is searching for xylem, and X wave phase when the insect is tasting to determine acceptability of a xylem cell (Backus 1988). B1s and XB1s waveforms (the latter described below) are occurring, respectively, during these times. Thus, fluid movements during B1s and XB1s are for tasting/testing.

The findings of Ruschioni et al. (2019) are important because they provide a plausible alternative mechanism for rinsing egestion during B1s or XB1s. Backus (2016) hypothesized that 'precibarial valve fluttering' (envisioned as the flap pivoting up and down on the valve fulcrum) based on Backus and McLean (1982) could cause turbulence in the area distal to the precibarial valve. The combined contributions of Ruschioni et al. (2019) and Ranieri et al. (2020) show that rinsing egestion is probably not propelled by valve 'fluttering' per se, but by valve-related turbulence, perhaps combined with putative cibarial quivering.

Two circumstances can be envisioned whereby precibarial turbulence could cause egestion of small amounts of fluid out the stylet tips. First, the insect could 'voluntarily' egest fluids by a combination of cibarial quivering and valve opening to cause outward-directed turbulence. Like sniffing in olfaction, frequent passage of fluids across gustatory sensilla prevents neuronal desensitization. Fluid could thus be leaked ('dribbled') (in the dictionary sense of 'issuing sporadically and in small bits') from below the valve and out the stylets. Second, when the flap of the valve is coated with obstructing microbes and biofilm that affixes it in a flattened, open position (Backus and Morgan 2011), it is likely that its check valve function could be impaired, preventing proper swallowing. In that case, vigorous attempts to open the valve could ensue. If the biofilm is small, turbulence combined with cibarial quivering could unblock the valve and egest small amounts of biofilm from both above and below the valve, thus contributing to inoculation of *X. fastidiosa*.

In summary, considering all evidence together, B1s during Pathway very likely represents a rapidly alternating sequence of events. First, uptake of tiny amounts of fluid (probably a mixture of saliva and plant juices) into the precibarium occurs by cibarial

quivering with the valve held open. Fluid is probably passed back and forth ('swished') across precibarial chemosensilla, initially the distal (D) sensilla then, if acceptable, across the P sensilla to taste/test the chemical contents of cells (Backus 1988). Second, swishing is followed by release of those small amounts of fluid out the stylet tips (rinsing egestion, or dribbling) via cibarial quivering and/or precibarial turbulence (Backus 2016). Light obstruction of the valve by microbial biofilm would cause more swishing and dribbling, contributing to inoculation of small amounts of *X. fastidiosa* into parenchyma, mesophyll, and immature xylem cells along the stylet pathway while the insect is searching for a mature xylem cell.

Type B2

This is a stereotypical, crescent-shaped (at lower Ri levels) series of short, triangular peaks (Fig. 4D). Rapid, in-out 'chiseling' movements of the maxillary stylet tips against the hardened wall of the salivary sheath have been observed in transparent artificial diet (Joost et al. 2006) and histologically in grape tissues (Backus et al. 2009). Electronically, B2 or (a smaller, shorter version, B2m) often occurs at the bottom of a 'trench' in waveform voltage at lower Ri levels, indicating stylet protraction into a xylem cell prior to chiseling and then subsequent retraction, and more chiseling. Spatially, B2 corresponds to a large blob of hardened sheath saliva at the junction where the sheath diverts into a new branch (Backus et al. 2009). Thus, stylet chiseling allows the insect to punch a hole through the already-solidified sheath wall and either extend stylets to lengthen a sheath branch in one direction, or make a new branch in a direction oblique to that of the previous branch (Joost et al. 2006). B2 is usually performed after testing/tasting of rejected, immature xylem cells (Backus et al. 2005, 2009). Thus, B2 is an important waveform behaviorally, because it indicates further searching for a xylem cell acceptable for ingestion and (usually) a branched salivary sheath.

X Wave Phase

An X wave is a species-specific, complex set of stereotypically repeating waveforms that can be seen in many hemipteran (and almost all auchenorrhynchan) EPG recordings (Backus et al. 2019). X waves represent key steps in final ingestion cell acceptance. In the case of aphids, the original 'X wave' term was coined for a distinctive appearance of (what are now called) waveforms C and pd, representing first contact with phloem sieve elements. These early studies used an AC monitor at Ri 10^6 Ohms (McLean and Kinsey 1967, Scheller and Shukle 1986). Today we understand that not all aphid species have distinctive-appearing waveforms preceding phloem ingestion. Those that do have a pre-phloem pd that appears distinctly different from pathway pd's. Such 'phloem-pd's' recently have been characterized and correlated using DC EPG at Ri 10^9 Ohms (Tjallingii and Gabryś 1999, Jimenez et al. 2020). Thus, when they occur, these distinctive X waves or phloem pd's provide definitive evidence that the stylets have entered an ingestion cell. In most cases, such as in aphids (Jimenez et al. 2020), many auchenorrhynchans (Wayadande and Nault 1993, Carpane et al. 2011), and some heteropterans (Cervantes et al. 2016, Lucini and Panizzi 2018), the ingestion cells are always phloem sieve elements. However, in the case of sharpshooters, the ingestion cell is a mature xylem tracheary element (Backus et al. 2009). A complete sharpshooter X wave includes both families XC and XN.

Family XC

This family represents fluid uptake, discharge egestion (XC1), and trial ingestion (XC2) (i.e., swallowing of large amounts of fluid from the entire buccal cavity, but for short durations).

Type XC1 (Miranda Xc)

Each XC event begins with few to many very tall, narrow, straight-walled and abrupt peaks (Fig. 5A–C). Thus, in cicadellines like *G. atropunctata*, XC1 peaks clearly mark the end of pathway/B1 and the start of X wave phase (Cervantes and Backus 2018). In contrast, in proconiine sharpshooters like *Homalodisca* spp., a clear XN-appearing event occurs at the end of pathway/B1 and XC does not begin until after that XN (Backus et al. 2009).

XC1 peaks are usually tall and thin (1/4 to 1/2 the duration of an XC2 plateau, or if the same duration then taller; Fig. 5C). XC1 peaks are emf-dominated with almost no R component (Cervantes and Backus 2018). Therefore, XC1 is likely caused by streaming potentials (Dugravot et al. 2008) generated by rapid fluid movement through the narrow, capillary-like food canal in the stylets. All of the evidence described above for streaming potentials and fluid flow applies for XC1, but even more forcefully and with greater volume. Fluid movement is driven by strong uplift then dropping of the cibarial diaphragm (Dugravot et al. 2008), causing negative then positive pressure (respectively) in the buccal cavity, which in turn pulls fluids inward (uptake) then rapidly propels them outward (egestion) from the stylet tips (Backus and Morgan 2011).

Because peak amplitude generated by streaming potentials is proportional to the degree of uplift of the cibarial diaphragm (Dugravot et al. 2008), the tallest XC1 peaks likely represent nearly maximum uplift of the diaphragm, to rapidly bring fluids from the plant into the full length of the buccal cavity. As described below under XC2, a steady voltage level after the rise (causing a flat top to XC2) is correlated with filling of the cibarium. Thus, a rapid drop of the XC1 peak means the diaphragm is lifted up but then immediately dropped, likely expelling the full volume of the precibarium and part or all of the cibarium out the stylet tips (Backus 2016, Backus et al. 2019, E. A. Backus, unpublished data).

High-amplitude XC1 peaks at the start of X waves probably represent the first uptake of fluids from a mature xylem cell because the strongly negative pressure potential of xylem sap requires very strong suction by the cibarial diaphragm (see Backus and Shih 2020 for comparison of XC1 and B1p). It has been proposed (Backus 2016) that subsequent rapid voltage drop represents rapid expulsion of fluids while the precibarial valve is held open, allowing fluid to flow out the stylet tips and back into the xylem cell. Thus, XC1 is likely to be the mechanism of forceful, 'discharging egestion' of all fluids in the precibarium, especially to clear out biofilm obstructions of the cibarium and precibarium prior to ingestion (Backus and Morgan 2011). Colloquially, XC1 can be thought of as uptake of fluid and 'spitting' (in the dictionary sense of 'forcefully ejecting something from the mouth') such fluid out the stylet tips. Accordingly, XC1 represents the second mechanism of *X. fastidosa* inoculation. Because its egestate is injected directly into a xylem cell plus likely larger in volume and thus will hold more bacterial cells, discharging egestion is likely to be a more etiologically important mechanism for bacterial inoculation than rinsing egestion.

Type XC2 (Miranda Xi)

During the X wave, short events of a waveform similar to C2 (but lasting <5 min; see description and correlations below), termed XC2

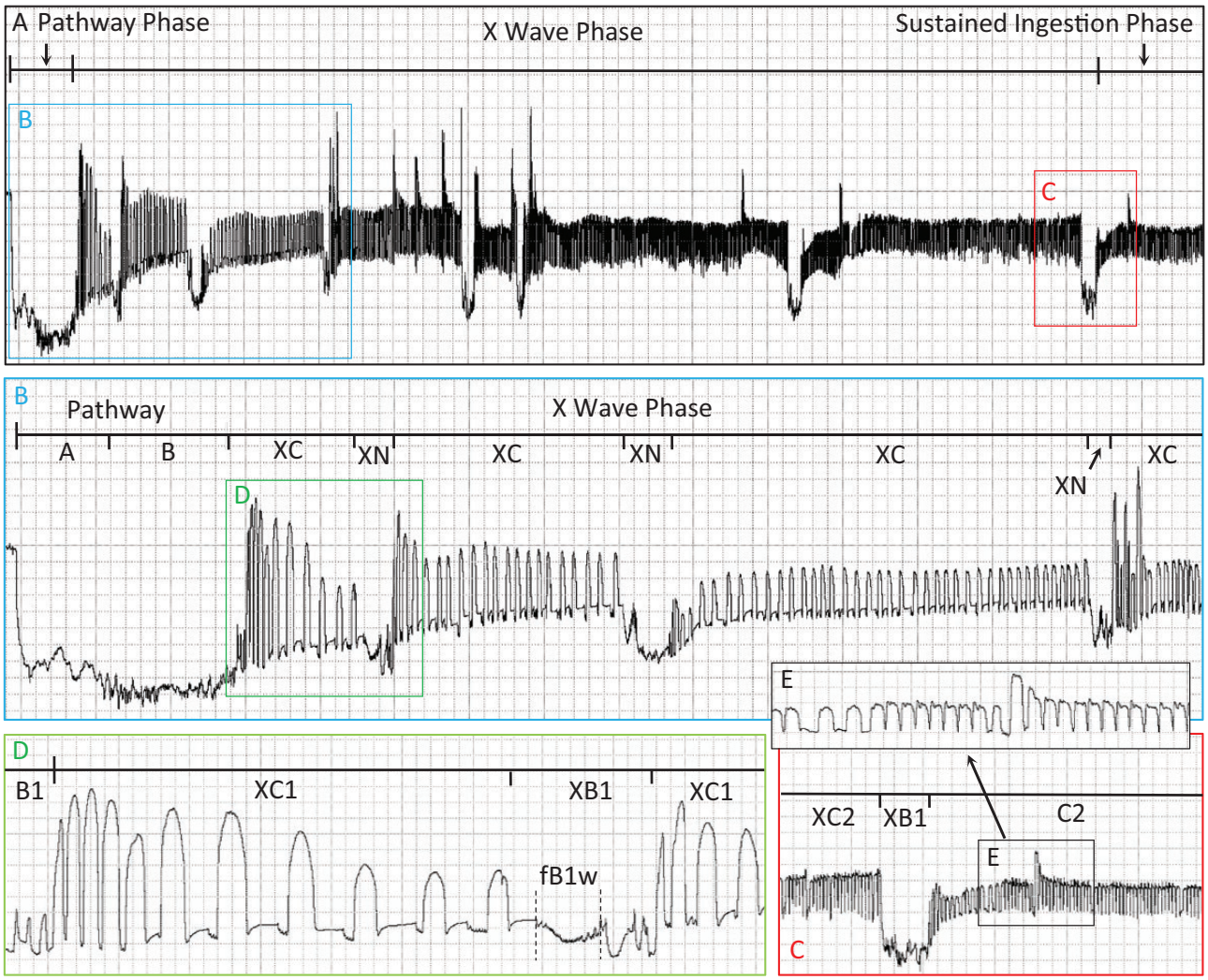

Fig. 5. Compressed examples of pathway and X wave phases, with certain sections expanded; from previously unpublished waveforms of *G. atropunctata*. (A) Waveform overview recorded using Ri 10^9 Ohms and 50 mV AC applied signal. (B) Expansion of pathway and early X waves from box labeled B in part A. (C) Expansion of later X waves from box labeled C in part A. (D) Further expansion of early X wave from box labeled D in part B. Windaq compression of part A is 45 (9 seconds per vertical division). Windaq compression of parts B, C, D, and E is 3 (0.6 seconds per division). Windaq gain is 4× in all views.

(Fig. 5D and E) are interspersed among XB1 events, described below. Termed trial ingestion (Crane 1970, Almeida and Backus 2004), these short XC2 events of ingestion or 'sipping' (to 'drink fluid in small quantities') are a signature of the X wave. As demonstrated by video recording of cibarial diaphragm movements correlated with EPG, repeated plateaus like XC2 and C2 (see below) occur when the cibarial diaphragm is either slowly lifted and/or held (during the flat top of the plateau) as the cibarium fills (Dugravot et al. 2008). Later, asymmetrical release of the diaphragm, combined with closure of the precibarial valve (functioning as a pressure-sensitive check valve) (Backus 1988, Ruschioni et al. 2019), allows fluids to be swallowed into the pharynx, then esophagus, and then midgut without egestion from the stylet tips. Thus, XC2 represents cibarial pumping and ingestion (defined as swallowing of fluids past the true mouth, i.e., the opening to the pharynx from the cibarium; Backus 2016, Backus et al. 2019). It is thought that these trial ingestion events allow the insect to test the strength of the mechanical seal of the salivary sheath into the xylem cell wall, to support longer-term pumping (Backus et al. 2012). Trial ingestion only occurs in mature xylem cells and defines a complete (as opposed to partial) X wave (Backus et al. 2009).

Family XN (Miranda N)

Sharpshooter XN was originally identified as N in a study using an AC monitor at Ri 10^6 Ohms (Backus et al. 2005). Figures in that paper show N with a distinctive, positive-oriented appearance above the very small XC2 waveform (then termed C). N was renamed XN in a later study using the AC-DC Correlation Monitor recording at 10^7, 10^8, or 10^9 Ri, when the sharpshooter X wave was identified (Backus et al. 2009). The XN family represents tasting/testing the chemical and mechanical suitability of and accepting a mature xylem cell, plus achieving a strong salivary sheath connection to the cell. Behaviors represented include salivation plus fluid uptake, swishing, and egestion (primarily rinsing egestion) of small amounts of mixed saliva and plant fluid to test/taste cell contents for acceptance. In *Homalodisca* spp., an XN-like waveform (termed a 'partial X wave') occurs at the end of pathway.

Type XB1

This waveform is the same in appearance as B1 above (during pathway), but is exclusively performed in mature xylem cells (Fig. 5C and D), to taste and test the chemical constituents of the xylem.

XB1: Subtype fB1w

B1w represents salivation (Joost et al. 2006), so 'fuzzy' B1w (Fig. 5D) probably represents salivation with a high-frequency component of unknown meaning (but perhaps pumping of the salivarium, or cibarial quivering?), superimposed on top. fB1w probably builds stronger anchoring of the salivary sheath to the xylem cell wall because successive events of XN have been shown to thicken the sheath lining in the xylem (Backus et al. 2009, E. A. Backus, unpublished data). This X wave subtype is considered diagnostic for an X wave.

XB1: Subtype XB1s

Similar in appearance to pathway B1s but often more amorphous in appearance (Fig. 5C and D), XB1s is usually not exclusively spikelet bursts and waves, but can include irregular regions. XB1s occurs exclusively during an XN event. Like B1s, XB1s is thought to represent rapid uptake and expulsion of tiny amounts of fluid into and out of the buccal cavity, perhaps simultaneously with watery salivation. Therefore, such uptake and rinsing egestion again can be thought of as swishing and dribbling, but only when the stylet tips are in xylem cells.

XB1: Subtype XB1p

Similar in appearance to pathway B1p described above, but occurring only in XN, thus in xylem cells (not shown). While uncommon in previously published recordings, this subtype was very common in recordings of *K. paulula*, as described more fully in Backus and Shih (2020).

Sustained Ingestion Phase

Family C

Sustained, long-duration cibarial pumping is family C; consumption (ingestion) of xylem sap for nutrition.

Type C2 (Miranda Xi)

C2 is similar in appearance to XC2, but much longer in duration (usually each event lasts >5 min to several hours) (Backus et al. 2005). Plateaus are stable in appearance, not evolving as in XC2. C2 ingestion has been correlated with watery excretory droplet formation and pH typical of xylem (Backus et al. 2005) as well as cibarial pumping (Dugravot et al. 2008). Thus, C2 represents sustained ingestion of xylem sap because it also has been histologically correlated with stylet tips in a mature xylem cell (Backus et al. 2005, 2009; Dugravot et al. 2008).

Family G

This is a 'resting' waveform (not shown) that is similar in appearance to C2, but with widely spaced plateaus that have distinctive 'ruffles' or short spike bursts on top of each plateau (Cervantes and Backus 2018, Backus and Shih 2020). G always follows XC2 or C2 without change in amplitude. It has been correlated with stylet tips still in a xylem cell (Backus et al. 2009), therefore is suspected to represent cessation of ingestion/pumping from a xylem cell but with occasional cibarial quivering to bring fluid into the precibarium for tasting/testing.

Other Waveforms

Family D

Types D1 and D2

These represent unknown behaviors, possibly stylets motionless or slowly moving.

Inoculation of *Xylella fastidiosa* in Xylem During Sharpshooter Stylet Probing

When the stylets enter a xylem cell, the insect salivates into the cell, then takes up combined saliva and xylem sap into its functional foregut where it 'swishes' the fluids around via combined cibarial quivering and precibarial valve movements. Swished fluids are tasted using gustatory chemosensilla lining the precibarium (Backus 1988) and probably simultaneously (both mechanically and enzymatically) loosen bacteria colonizing the buccal cavity. The insect then expels (egests) the fluid out its stylets (rinsing egestion during XB1s or discharge egestion during XC1), thereby inoculating *X. fastidiosa* into the plant's xylem cells. The existence of this combined salivation and egestion behavior and its role in expelling *X. fastidiosa* cells from the stylet tips has been solidly proven (Backus and Morgan 2011). These combined behaviors are proposed to be represented by XB1s and XC1 when they are performed alternately with trial ingestion (XC2) during the sharpshooter X wave in mature xylem cells (Backus et al. 2009, Backus and Morgan 2011). Recently published preliminary results using qPCR to detect bacteria injected after two to four X waves performed in the same xylem cell support that the X wave represents inoculation of *X. fastidiosa* into xylem cells (Backus et al. 2018b); further repetitions of this experiment are underway.

Types of EPG Experiments

The details of waveform appearances and waveform names presented above were developed in large part to discover and define the behavioral mechanisms of acquisition and inoculation of *X. fastidiosa* during sharpshooter stylet probing. Studies such as waveform characterization, correlation, and waveform libraries are known as qualitative EPG studies, because they are performed to define the biological meanings of waveforms and do not involve statistically comparing among experimental treatments. Now that mechanisms of *X. fastidiosa* transmission are understood and the waveforms described (herein, Backus 2016, Cervantes and Backus 2018, Krugner et al. 2019, Backus and Shih 2020), EPG can be used as a tool for development of novel tactics of disease and vector management. Such development requires quantitative comparisons of stylet probing behavior under multiple treatments, for example, chemical compounds or putatively resistant genotypes of plants (Yorozuya 2017, Chen et al. 2019, Pacheco et al. 2020).

Recommended Sharpshooter (and Spittlebug) Waveforms to Measure for Quantitative Experiments

Table 1 provides our recommendations (bold plus underlined waveform names) for level of waveform detail to be used for waveform measurement (or annotation) of quantitative studies. Hereafter, we provide justification for our recommendations. Evidence for these conclusions are explained in detail in the above narrative.

Most pathway waveforms are not essential for understanding *X. fastidiosa* transmission. However, we have found that B2 is a very useful waveform because it represents salivary sheath branching as the insect abandons an unacceptable xylem cell and renews its search for an acceptable cell. Thus, long durations of pathway (measured as P) with numerous, interspersed B2 events shows that an insect is having difficulty finding and accepting a mature xylem cell for sustained ingestion. As described more in Backus and Shih (2020), we also recommend measuring B1p during pathway.

X wave components are especially important for understanding the probability of insects inoculating *X. fastidiosa*. Because XN is mostly composed of XB1 (including XB1s, fB1w, and XB1p),

all of which likely play some role in inoculation, we recommend simplifying measurement by using XN. Also, because XC1 (inoculation) and XC2 (likely acquisition) each play different roles in transmission, they should be measured separately. C2 likely has the greatest importance for acquisition, while G probably plays no role in transmission; therefore, they should be separately measured. It is possible that rare, non-X wave interruptions in sustained ingestion (C2) called N might also play a role in inoculation, but less likely than XN because bacteria in the functional foregut are likely to be previously expelled during X waves. Therefore, we recommend measuring N separate from XN. R (resting stylets) and G should be measured separately from C2 to ensure that ingestion-like durations are not overestimated if the three were combined. Finally, as shown by Cervantes and Backus (2018), unusual waveforms like D and SR can occur when insects are debilitated or on nonhost plants; therefore, when recorded, they should be measured but kept separate from ingestion and interruption waveforms. Several useful waveforms described above are not separately identifiable using the Miranda naming convention.

In conclusion, EPG waveforms of Western Hemisphere vectors of *X. fastidiosa* are now well characterized and their biological meanings understood. It is especially important that the waveforms representing the behaviors that underlie bacterial inoculation have been identified. Before quantitative EPG studies are performed to aid in development of resistance to *X. fastidiosa* inoculation, it will be valuable to characterize the waveforms of sharpshooters outside the Western Hemisphere. Backus and Shih (2020) asks and answers whether the descriptions herein are globally applicable to species elsewhere in the world.

Acknowledgments

The editorial suggestions of James Throne (ARS Parlier) plus four anonymous reviewers were greatly appreciated. This work was supported in part by the Ministry of Science and Technology Foundation (grant number MOST 108-2321-B-005-007) and in part by the Council of Agriculture Foundation (grant number 107AS-4.1.1-CI-C1) of the Republic of China (to H.-T.S.), and by in-house funds from USDA-ARS (2034-22000-010-00D) (to E.A. B.).

References Cited

Almeida, R. P. P., and E. A. Backus. 2004. Stylet penetration behaviors of *Graphocephala atropunctata* (Signoret) (Hemiptera, Cicadellidae): EPG waveform characterization and quantification. Ann. Entomol. Soc. Am. 97: 838–851.

Almeida, R. P. P., M. J. Blua, J. R. S. Lopes, and A. H. Purcell. 2005. Vector transmission of *Xylella fastidiosa*: applying fundamental knowledge to generate disease management strategies. Ann. Entomol. Soc. Am. 98: 775–786.

Backus, E. A. 1988. Sensory systems and behaviours which mediate hemipteran plant-feeding: a taxonomic overview. J. Insect. Physiol. 34: 151–157, 159–165.

Backus, E. A. 2016. Sharpshooter feeding behavior in relation to transmission of *Xylella fastidiosa*: a model for foregut-borne transmission mechanisms, pp. 173–194. *In* J. K. Brown (ed.), Vector-mediated transmission of plant pathogen. American Phytopathological Society Press, St. Paul, MN.

Backus, E. A., and W. H. Bennett. 1992. New AC electronic insect feeding monitor for fine-structure analysis of waveforms. Ann. Entomol. Soc. Am. 85: 437–444.

Backus, E. A., and W. H. Bennett. 2009. The AC-DC Correlation Monitor: new EPG design with flexible input resistors to detect both R and emf components for any piercing-sucking hemipteran. J. Insect Physiol. 55: 869–884.

Backus, E. A., and D. L. McLean. 1982. The sensory systems and feeding behavior of leafhoppers. I. The aster leafhopper, *Macrosteles fascifrons* Stål (Homoptera: Cicadellidae). J. Morphol. 172: 359–378.

Backus, E. A., and D. L. McLean. 1983. Behavioral evidence that the precibarial sensilla of leafhoppers are chemosensory and function in host discrimination. Entomol. Exp. Appl. 37: 219–228.

Backus, E. A., and D. J. Morgan. 2011. Spatiotemporal colonization of *Xylella fastidiosa* in its vector supports the role of egestion in the inoculation mechanism of foregut-borne plant pathogens. Phytopathology. 101: 912–922.

Backus, E. A., and H. T. Shih. 2020. Do sharpshooters from around the world produce the same EPG waveforms? Comparison of waveform libraries from *Xylella fastidiosa* vectors *Kolla paulula* from Taiwan and *Graphocephala atropunctata* from California. J. Insect Sci. In press.

Backus, E. A., M. J. Devaney, and W. H. Bennett. 2000. Comparison of signal processing circuits among seven AC electronic monitoring systems for their effects on the emf and R components of aphid (Homoptera: Aphididae) waveforms, pp. 102–143. *In* G. P. Walker and E. A. Backus (eds.), Principles and applications of electronic monitoring and other techniques in the study of homopteran feeding behavior. Thomas Say Publications in Entomology: proceedings. Entomological Society of America, Lanham, MD.

Backus, E. A., J. Habibi, F. Yan, and M. Ellersieck. 2005. Stylet penetration by adult *Homalodisca coagulata* on grape: electrical penetration graph waveform characterization, tissue correlation, and possible implications for transmission of *Xylella fastidiosa*. Ann. Entomol. Soc. Am. 98: 787–813.

Backus, E. A., A. R. Cline, M. S. Serrano, and M. R. Ellersieck. 2007. *Lygus hesperus* (Knight) Hemiptera: Miridae) feeding on cotton: new methods and parameters for analysis of non-sequential EPG data. Ann. Entomol. Soc. Am. 100: 296–310.

Backus, E. A., W. J. Holmes, F. Schreiber, B. J. Reardon, and G. P. Walker. 2009. Sharpshooter X wave: correlation of an electrical penetration graph waveform with xylem penetration supports a hypothesized mechanism for *Xylella fastidiosa* inoculation. Ann. Entomol. Soc. Am. 102: 847–867.

Backus, E. A., K. B. Andrews, H. J. Shugart, L. Carl Greve, J. M. Labavitch, and H. Alhaddad. 2012. Salivary enzymes are injected into xylem by the glassy-winged sharpshooter, a vector of *Xylella fastidiosa*. J. Insect Physiol. 58: 949–959.

Backus, E.A., M. Rangasamy, M. Stamm, H. J. McAuslane, and R. Cherry. 2013. Waveform library for chinch bugs (Hemiptera: Heteroptera: Blissidae): characterization of electrical penetration graph waveforms at multiple input impedances. Ann. Entomol. Soc. Am. 106: 524–539.

Backus, E. A., P. A. Lin, C. J. Chang, and H. T. Shih. 2016. Electropenetrography: a new diagnostic technology for study of feeding behavior of piercing-sucking insects. J. Taiwan Agric. Res. 65: 219–237.

Backus, E. A., F. A. Cervantes, L. Godfrey, W. Akbar, T. L. Clark, and M. G. Rojas. 2018a. Certain applied electrical signals during EPG cause negative effects on stylet probing behaviors by adult *Lygus lineolaris* (Hemiptera: Miridae). J. Insect Physiol. 105: 64–75.

Backus, E. A., F. A. Cervantes, J. Van De Veire, L. Burbank, and T. M. Perring. 2018b. Sharpshooter electropenetrography X wave represents the *Xylella fastidiosa* inoculation behaviors: update on evidence from systemic, symptomatic Pierce's disease infections induced after X waves, pp. 145–148. *In* Proceedings of the 2018 Pierce's disease research symposium. https://www.cdfa.ca.gov/pdcp/Documents/Proceedings/2018ResearchProgressRpts.pdf

Backus, E. A., F. A. Cervantes, R. Narciso Guedes, A. Y. Li, and A. C. Wayadande. 2019. AC-DC electropenetrography (EPG) for in-depth studies of oviposition and piercing-sucking feeding behaviors. Ann. Entomol. Soc. Am. 112: 236–248.

Carpane, P., A. Wayadande, E. A. Backus, W. Dolezal, and J. Fletcher. 2011. Characterization and correlation of new electrical penetration graph waveforms for the corn leafhopper (Hemiptera: Cicadellidae). Ann. Entomol. Soc. Am. 104: 515–525.

Cervantes, F. A., and E. A. Backus. 2018. EPG waveform library for *Graphocephala atropunctata* (Hemiptera: Cicadellidae): effect of adhesive, input resistor, and voltage levels on waveform appearance and stylet probing behaviors. J. Insect Physiol. 109: 21–40.

Cervantes, F. A., E. A. Backus, L. Godfrey, W. Akbar, and T. L. Clark. 2016. Characterization of an EPG waveform library for adult *Lygus lineolaris* and *Lygus hesperus* (Hemiptera: Miridae) feeding on cotton squares. Ann. Entomol. Soc. Am. 109: 684–697.

Chen, Y., X. Rong, Q. Fu, B. Li, and L. Meng. 2019. Effects of biochar amendment to soils on stylet penetration activities by aphid *Sitobion avenae* and planthopper *Laodelphax striatellus* on their host plants. Pest Manag. Sci. 76: 360–365.

Chuche, J., E. A. Backus, T. Denis, and N. Sauvion. 2017. First finding of a dual-meaning X wave for phloem and xylem fluid ingestion: characterization of *Scaphoideus titanus* (Hemiptera: Cicadellidae) EPG waveforms. J. Insect. Physiol. 109: 684–697.

Collar, J. L., and A. Fereres. 1998. Nonpersistent virus transmission efficiency determined by aphid probing behavior during intracellular punctures. Environ. Entomol. 27: 583–591.

Cornara, D., M. Saponari, A. R. Zeilinger, A. de Stradis, D. Boscia, G. Loconsole, D. Bosco, G. P. Martelli, R. P. P. Almeida, and F. Porcelli. 2017. Spittlebugs as vectors of *Xylella fastidiosa* in olive orchards in Italy. J. Pest Sci. (2004). 90: 521–530.

Cornara, D., E. Garzo, M. Morente, A. Moreno, J. Alba-Tercedor, and A. Fereres. 2018. EPG combined with micro-CT and video recording reveals new insights on the feeding behavior of *Philaenus spumarius*. PLoS One. 13: e0199154.

Crane, P. S. 1970. The feeding of the blue-green sharpshooter *Hordnia circellata* (Baker) (Homoptera: Cicadellidae). Entomology Dept., University of California, Davis, CA.

Dugravot, S., E. A. Backus, B. J. Reardon, and T. A. Miller. 2008. Correlations of cibarial muscle activities of *Homalodisca* spp. sharpshooters (Hemiptera: Cicadellidae) with EPG ingestion waveform and excretion. J. Insect Physiol. 54: 1467–1478.

Ebert, T. A., E. A. Backus, M. Cid, and A. Fereres. 2015. A new SAS program for behavioral analysis of electrical penetration graph data. Comput. Electron. Agric. 116: 80–87.

Fereres, A. 2016. Aphid behavior and the transmission of noncirculative viruses. *In* J. K. Brown (ed.), Vector-mediated transmission of plant pathogens. American Phytopathological Society Press, St. Paul, MN.

Jimenez, J., E. Garzo, J. Alba-Tercedor, A. Moreno, A. Fereres, and G. P. Walker. 2020. The phloem-pd: ad distinctive brief sieve element stylet puncture prior to sieve element phase of aphid feeding behavior. Arthropod Plant Interact. 14: 67–78.

Jones, M. 2014. Chapter 4 – Test equipment principles, pp. 235–380. *In* Building valve amplifiers, 2nd ed. Elsevier, Amsterdam.

Joost, P. H., E. A. Backus, D. Morgan, and F. Yan. 2006. Correlation of stylet activities by the glassy-winged sharpshooter, *Homalodisca coagulata* (Say), with electrical penetration graph (EPG) waveforms. J. Insect Physiol. 52: 327–337.

Krugner, R., M. S. Sisterson, E. A. Backus, L. P. Burbank, and R. A. Redak. 2019. Sharpshooters: a review of what moves *Xylella fastidiosa*. Austral Entomol. 58: 248–267.

Lucini, T., and A. R. Panizzi. 2018. Electropenetrography (EPG): a breakthrough tool unveiling stink bug (Pentatomidae) feeding on plants. Neotrop. Entomol. 47: 6–18.

Lucini, T., A. R. Panizzi, and E. A. Backus. 2016. Characterization of an EPG waveform library for redbanded stink bug, *Piezodorus guildinii* (Hemiptera: Pentatomidae), on soybean plants. Ann. Entomol. Soc. Am. 109: 198–210.

McLean, D. L., and M. G. Kinsey. 1964. A technique for electronically recording aphid feeding and salivation. Nature. 202: 1358–1359.

McLean, D. L., and M. G. Kinsey. 1967. Probing behavior of the pea aphid, *Acyrthosiphon pisum*. I. Definitive correlation of electronically recorded waveforms with aphid probing activities. Ann. Entomol. Soc. Am. 60: 400–405.

Miranda, M. P., A. Fereres, B. Appezzato-Da-Gloria, and J. R. S. Lopes. 2009. Characterization of electrical penetration graphs of *Bucephalogonia xanthophis*, a vector of *Xylella fastidiosa* in citrus. Entomol. Exp. Appl. 130: 35–46.

Pacheco, I. S., D. M. Galdeano, N. K. P. Maluta, J. R. S. Lopes, and M. A. Machado. 2020. Gene silencing of *Diaphorina citri* candidate effectors promotes changes in feeding behaviors. Sci. Rep. 10: 5992.

Pearson, C. C., E. A. Backus, H. J. Shugart, and J. E. Munyaneza. 2014. Characterization and correlation of EPG waveforms of *Bactericera cockerelli* (Hemiptera: Triozidae): variability in waveform appearance in relation to applied signal. Ann. Entomol. Soc. Am. 107: 650–666.

Powell, G., T. Pirone, and J. Hardie. 1995. Aphid stylet activities during potyvirus acquisition from plants and an in vitro system that correlate with subsequent transmission. Eur. J. Plant Pathol. 101: 411–420.

Purcell, A. H. 1997. *Xylella fastidiosa*, a regional problem or global threat? J. Plant Pathol. 79: 99–105.

Ranieri, E., G. Zitti, P. Riolo, N. Isidoro, S. Ruschioni, M. Brocchini, and R. P. P. Almeida. 2020. Fluid dynamics in the functional foregut of xylem-sap feeding insects: a comparative study of two *Xylella fastidiosa* vectors. J. Insect Physiol. 120: 103995.

Ruschioni, S., E. Ranieri, P. Riolo, R. Romani, R. P. P. Almeida, and N. Isidoro. 2019. Functional anatomy of the precibarial valve in *Philaenus spumarius* (L.). PLoS One. 14: e0213318.

Sandanayaka, W. R. M., and E. A. Backus. 2008. Quantitative comparison of stylet penetration behaviors of glassy-winged sharpshooter on selected hosts. J. Econ. Entomol. 101: 1183–1197.

Sandanayaka, W. R. M., A. Chhagan, and P. Ramankutty. 2007. Host plant testing of the spittle bug *Carystoterpa fingens* by stylet penetration behaviour. N. Z. Plant Prot. 60: 78–84.

Sandanayaka, W. R. M., Y. Jia, and J. G. Charles. 2012. EPG technique as a tool to reveal host plant acceptance by xylem sap-feeding insects. J. Appl. Entomol. 137: 519–529.

Scheller, H. V., and R. H. Shukle. 1986. Feeding behavior and transmission of *Barley yellow dwarf virus* by *Sitobion avenae* on oats. Entomol. Exp. Appl. 40: 189–195.

Spiller, N.J., L. Koenders, and W. F. Tjallingii. 1990. Xylem ingestion by aphids - a strategy for maintaining water balance. Entomol. Exp. Appl. 55: 101–104.

Tjallingii, W. F. 1978. Electronic recording of penetration behaviour by aphids. Entomol. Exp. Appl. 24: 721–730.

Tjallingii, W. F. 1985a. Electrical nature of recorded signals during stylet penetration by aphids. Entomol. Exp. Appl. 38: 177–186.

Tjallingii, W. F. 1985b. Membrane potentials as an indication for plant cell penetration by aphid stylets. Entomol. Exp. Appl. 38: 187–193.

Tjallingii, W. F. 1988. Electrical recording of stylet penetration activities. Chapter 8.8, pp. 95–108. *In* A. K. Minks and P. Harrewijn (eds.), Aphids, their biology, natural enemies and control, Vol. 2B. Elsevier, Amsterdam, The Netherlands.

Tjallingii, W. F. 2000. Comparison of AC and DC systems for electronic monitoring of stylet penetration activities by homopterans, pp. 41–69. *In* G. P. Walker and E. A. Backus (eds.), Principles and applications of electronic monitoring and other techniques in the study of homopteran feeding behavior. Thomas Say Publications in Entomology: proceedings. Entomological Society of America, Lanham, MD.

Tjallingii, W. F., and T. H. Esch. 1993. Fine-structure of aphid stylet routes in plant-tissues in correlation with EPG signals. Physiol. Entomol. 18: 317–328.

Tjallingii, W. F., and B. Gabryś. 1999. Anomalous stylet punctures of phloem sieve elements by aphids. Entomol. Exp. Appl. 91: 97–103.

Ullman, D. E., and D. L. McLean. 1986. Anterior alimentary canal of the pear Psylla, *Psylla pyricola* foerster (Homoptera, Psyllidae). J. Morphol. 189: 89–98.

Walker, G. P. 2000. Beginner's guide to electronic monitoring, pp. 14–40. *In* G. P. Walker and E. A. Backus (eds.), Principles and applications of electronic monitoring and other techniques in the study of homopteran feeding behavior. Thomas Say Publications in Entomology: proceedings. Entomological Society of America, Lanham, MD.

Wayadande, A. C., and L. R. Nault. 1993. Leafhopper probing behavior associated with maize chlorotic dwarf virus transmission to maize. Phytopathology. 83: 522–526.

Yorozuya, H. 2017. Analysis of tea plant resistance to tea green leafhopper, *Empoasca onukii*, by detecting stylet-probing behavior with DC electropenetrography. Entomol. Exp. Appl. 165: 62–69.